DEVELOPING CRAMER-RAO LOWER BOUNDS TO GAUGE EFFECTIVENESS OF UEWR TARGET TRACKING FILTERS*

Thomas H. Kerr, CEO/Principal Investigator†
TeK Associates, Lexington, MA 02420

Abstract

A Cramer-Rao Lower Bound (CRLB) evaluation methodology is developed and used within the UEWR (Upgraded Early Warning Radar) strategic radar scenario of National Missile Defense (NMD) to gauge the effectiveness of target tracking filters. The particular mechanization offered here adaptively handles the Signal-to-Noise ratio (SNR) at a variable rate whenever it becomes available as a consequence of the behavior of the radar resource "scheduler," track initialization procedure, detection threshold setting, and other internal radar signal processing considerations and options (such as possible initiation of coherent integration to enhance the effective SNR available). Accommodating a fluctuating SNR available at varying step sizes allows our calculated CRLBs to realistically reflect the actual situation rather than merely assume that SNR data samples are available at a constant fixed rate. To our knowledge, this is the first CRLB application that includes use of per pulse SNR's in this manner for greater realism to more accurately reflect and accommodate what occurs in practice (and, likewise, to also match the situation arising in realistic simulations).

1. Introduction

A brief overview is provided in Sec. 2 of the Cramer-Rao inequality of *statistics* as it arises in this nonlinear estimation problem of radar target tracking. Sec. 3 reviews the underlying system structure at a high level and summarizes the result of extrapolating the linear estimation approach of ordinary Kalman filtering to an Extended Kalman Filter (EKF), applicable for state estimation in this nonlinear system. The discussion here takes advantage of the considerable commonality between many aspects of an EKF mechanization and that of a CRLB mechanization yet still draws the appropriate distinctions. Sec. 4.1 discusses the additional detailed modeling considerations and calculations performed to match up CRLB calculation to the radar target tracking problem. Sec. 4.2 describes the constituent components of our particular CRLB implementation and provides the theoretical justification based on structure of the measurements that it encompasses. A nonlinear filtering application example in National Missile Defense (NMD) strategic defense radar target tracking is used to demonstrate the utility of this new CRLB evaluation formulation. Illustrative CRLB results are analyzed in Sec. 5 in making comparisons to averaged EKF output in order to gauge the target tracking performance of this particular EKF against the best that can be achieved by **any** sequential estimator (according to the mild conditions of Sec. 4). Sec. 6 summarizes our results and offers suggested improvements and lists other strategic and tactical target tracking scenarios that may benefit from detailed CRLB evaluations.

2. CRLB's for Gauging the Utility of Target Tracking Filters

Under the standard assumption that the *estimator is unbiased* [1], then the familiar form of Cramer-

*Research funded by MITRE Project 039840000-N0 under Air Force Contract No. F19628-94-C-0001. Approved for public release; distribution is unlimited.

[1] The bias referred to here is inherent to a particular estimator (like the $1/N$ factor present in a *maximum likelihood estimate* of the variance for a Gaussian random variable rather than the $1/(N-1)$ appearing in the well-known preferred **unbiased** estimator of the variance, a distinction that is insignificant for large N but very important for small N) and is generally NOT directly related to any underlying fundamental biases being present in the physical application (such as a bias due to other causes such as a terrestrial radar's residual elevation distortion bias incurred as a consequence of the atmospheric lens effect) or arising for reasons other than the structure of the estimator being employed within a particular application.

Rao inequality encountered or invoked most frequently is:

$$E[(x-\hat{x})(x-\hat{x})^T|x] \geq \left[-\mathrm{E}\{(\tfrac{\partial}{\partial x})^T(\tfrac{\partial}{\partial x})\ln\{p(z|x)\}\}\right]^{-1} \equiv \mathcal{I}^{-1}, \quad (1)$$

where the inequality here for these matrices is interpreted in the matrix positive semi-definite sense (i.e., $A \geq B \Longrightarrow A-B \geq 0$). Please see [3] and its references for details. It is this form [2] (under the widely invoked assumption that the estimator bias is non-existent or negligible) that has a RHS that is independent of the particular estimator being used and that may be compared to a wide variety of distinctly different estimators as a single relative gauge throughout. The CRLB methodology is used here to gauge the quality of filter performance in the tracking task.

The above Cramer-Rao inequality arises in seeking to estimate an unknown parameter x using **any** estimator $\hat{x}$ and the measurement $z(t)$, referenced above and available from the sensor as a time record, must be a non-trivial function of the unknown parameter x as

$$z(t) = h(x,t,v(t)). \quad (2)$$

In the above, $p(x|z)$ is the conditional probability density function (pdf) of x given all the measurements z, and $v(t)$ is the measurement noise. In exoatmospheric target tracking, x is deterministic and satisfies a known nonlinear ordinary differential equation and v is additive Gaussian white noise of known covariance intensity, hence $p(z|x)$ is known.

Other bounds exist such as that of Zacks and Barankin and information theoretic bounds and the interrelationship is known [4], [5]. The CRLB was selected for use here as the familiar bound most appropriate for this NMD application because it matches the situation and is tractable. A high-level overview of the CRLB methodology and its benefits and limitations follow.

The simulation performance of any estimator selected for the particular application can be "gauged for goodness" as ascertained by its relative proximity to the CR lower bound. Alternate estimator designs can be traded-off by proximity to the lower bound (as the best that can be done, where being closer is interpreted as being "better") versus computational burden associated with implementation. It is precisely this aspect of CRLB usage that is of interest in most nonlinear filtering applications.

The CR inequality of Eq. 1 provides a lower bound on the mean-square estimation error achievable. No matter what sequential estimator is ultimately selected, none can do better than what the rock-bottom nonnegative CRLB indicates to be the case (within certain common sense limitations to be discussed next). Obviously, as in any other simulation approach, CR bounding techniques are susceptible to inadvertent or intentional modeling errors or oversights (e.g., use of over simplified "truth" models or the intentional or inadvertent omitting of relevant states or instances of inadequate parameter selection). In such cases, the calculated CRLB can be either too high or too low but should be correct when the significant states are correctly included in the model and the proper parameters are used.

Whether the CR bound is tight or not is another question that depends on problem structure for an answer and which is discussed in [6], [3, after Eq. 3b]. For nonlinear estimators of interest here, even though the noise is additive and Gaussian (as fulfills the first requirement for estimators to achieve their CRLB), the radar measurements received violate the second condition by NOT being a linear function of the state parameter (cf., Eq. 10 and Eq. 19) as is also required for actually **achieving** the CRLB. (The CRLB being achieved means that the error of estimation term on the LHS of Eq. 1 touches the CRLB term on the RHS by satisfying the indicated inequality as an exact equality.) So the lower bound should not generally be achievable (hence this CRLB is NOT expected to **exactly** match the average sampled tracking error variance compiled from N Monte-Carlo trials).

The CRLB is of particular interest when the physics or geometric structure underlying a particular parameter estimation problem of interest doesn't support estimation objectives to the degree of accuracy sought or specified as the goal so that the estimator isn't unfairly blamed for what is beyond its control. That such an unfortunate circumstance is present in a particular application is reflected by a corresponding increase in size of the CRLB as a consequence of the fundamental decrease in the absolute accuracy achievable. The CRLB used here by adapting to a time-varying SNR to realistically correspond to fluctuating PRF and other underlying signal processing is an enhancement of the fundamental method-

[2] The summarizing notation $\mathcal{I}$ appearing on the Right Hand Side (RHS) in Eq. 1 is known as the *Information matrix* prior to matrix inversion, after which the entire expression is the so-called or so-designated Cramer-Rao Lower Bound (CRLB), which can be numerically evaluated.

	Propagate Step	Update Step
COVARIANCE	$P_{k\|k-1} = \Phi(k,k-1)P_{k-1\|k-1}\Phi^T(k,k-1) + Q_k$	$P_{k\|k} = [I - K_k H_k]P_{k\|k-1}[I - K_k H_k]^T + K_k R K_k^T$
FILTER GAIN	$K_k = P_{k\|k-1}H_k^T[H_k P_{k\|k-1} H_k^T + R]^{-1}$	
FILTER	$\hat{x}_{k\|k-1} = \hat{x}_{k-1\|k-1} + \int_{t_{k-1}}^{t_k} f(\hat{x}_{\tau\|t_{k-1}})\, d\tau$	$\hat{x}_{k\|k} = \hat{x}_{k\|k-1} + K_k(z_k - h(\hat{x}_{k\|k-1}))$

Table 1: Extended Kalman Filter Implementation/Mechanization Equations

ology that evolved in [7]–[10], as tailored to this NMD radar application using the conventions laid out in [11].

3. Commonality between EKF and CRLB

3.1 The Common System Model utilized by Both

The standard linear dynamical system for which Kalman-type filters are designed has a discrete-time representation consisting of an n-dimensional state vector x_k and an m-dimensional measurement vector z_k of the following well-known form:

$$\text{System} : x_{k+1} = \Phi(k+1,k)x_k + w_k, \quad (3)$$

$$\text{Measurement} : z_k = H_k x_k + v_k, \quad (4)$$

with initial condition $x(0) \sim \mathcal{N}(\bar{x}(0), P(0))$ (Gaussianly distributed, with known mean $\bar{x}(0)$ and covariance matrix $P(0)$) and where $\Phi(k+1,k)$ is the known *transition matrix* and the process and measurement noises, w_k and v_k, respectively, are zero mean, white Gaussian noises (independent of the Gaussian initial condition) of known covariance intensity levels Q_k and R, respectively. The three symmetric matrices $P(0)$ and Q_k must be *positive semi-definite* and R must usually be *positive definite*. The usual conditions of observability/controllability (or less restrictive detectability/stabilizability conditions) are assumed to be satisfied here by any appropriate application system of the form of Eqs. 3 and 4. The above regularity conditions being satisfied guarantee that the covariance calculations from the associated Riccati equation (to be defined below) will be well-behaved.

Eq. 3 above is a discrete-time difference equation (compatible with recursive implementation on a digital computer) that corresponds to the solution of an associated underlying continuous-time state variable differential equation (describing the system) of the form:

$$\frac{dx}{dt} = F(t)x + w'(t), \quad (5)$$

where the *transition matrix* for the general time-varying case of $F(t)$ is obtained by integration of the homogenous part of Eq. 5 over the time interval of interest prior to the next measurement becoming available for use by the filter. If $F(t)$ is constant, then the appropriate transition matrix simplifies to just an evaluation of the fairly well-known matrix exponential as

$$\Phi(k+1,k) = e^{F\Delta}, \quad (6)$$

where Δ is the appropriate time-step between measurements. Similarly, the appropriately exact discrete-time process noise covariance intensity level, Q_k, to use in the Kalman filter mechanization equations corresponding to Eq. 3 is obtained by integration of the known continuous-time process noise covariance intensity level, $Q_c(t)$, associated with the continuous-time white Gaussian noise $w'(t)$ of Eq. 5 as (Eq. 15 of Ref. 13 and Eq. 10 of Ref. 15):

$$Q_k = \int_{t_k}^{t_{k+1}} \Phi(t_{k+1},\tau)Q_c(\tau)\Phi^T(t_{k+1},\tau)\, d\tau, \quad (7)$$

where $\Delta = t_{k+1} - t_k$. (In seeking to track exoatmospheric targets, Q_c should be zero for the CRLB corresponding to no plant noise being present except for the practical consideration of a nominal nonzero tuning value [3] to keep the EKF filter bandwidth open and receptive to new measurements rather than ignoring them.)

The standard familiar Kalman filter implementation/mechanization equations for periodic measurements available every Δ units of time are well-known, as succinctly stated in Figs. 4.2-2 and 4.2-3 on p. 111 of Ref. 16.

The covariance update equation (Riccati Eq.) is

$$P_{k|k} = [I - K_k H_k]P_{k|k-1}$$

[3] The EKF tuning used in the nominal EKF within the Test Driver/ Software Algorithm Testbed (TD/SAT) as exhibited in Sec. 5 used tuning of 10^{-5} throughout a fictitious diagonal Q_c.

$$= [I - K_k H_k] P_{k|k-1} [I - K_k H_k]^T + K_k R K_k^T, \quad (8)$$

while the above two forms are mathematically equivalent, it is the more complex final expression (known as Joseph's form) that more effectively resists the deleterious effect of roundoff in machine computations (pp. 305-306 of Ref. 16) and is therefore the preferred implementation. More detail on the fundamentals of a linear Kalman filter estimator implementation and recommended steps to ease its software validation/checkout are provided in [13]–[15]. Although depicted as such for simplicity in Table 1, the Kalman filter (KF) usage is by no means restricted to just situations involving periodic availability of sensor measurements since a KF can handle asynchronous measurement availability of any known time spacing of measurements or even synchronized simultaneous measurements from several different sensors at a time and likewise for an EKF.

3.2 Primary Distinction in an EKF Mechanization

Mechanization of an *Extended Kalman Filter* can be applied to nonlinear situations [pp. 39-59 of Ref. 9] (such as are encountered in a more realistically detailed model of target complex trajectories). This is accomplished by linearizing (as the first two terms of a Taylor series expansion, involving a constant term and a 1^{st} derivative term, known as the *Jacobian*) of either the system equation or measurement equation (or both if each is nonlinear) as evaluated about the current state estimate, $\hat{x}(k)$, as obtained via an on-line mechanization of the Kalman filter implementation equations of Figs. 4.2-2 and 4.2-3 on p. 111 of Ref. 16 (corresponding to an assumed underlying model of the form of Eqs. 3 and 4) even though the actual system under consideration is now of the more general nonlinear continuous-time system/discrete-time measurement form

$$\text{System} : \frac{dx(t)}{dt} = f(x(t), t) + w(t), \quad (9)$$

$$\text{Measurement} : z_k = h(x_k, k) + v_k, \quad (10)$$

where $f(\cdot)$ and $h(\cdot)$ are the particular nonlinearities that are actually encountered in appropriately modeling the particular application (and are identified for NMD in Sec. 4).

The explicit implementation equations for an EKF [4], as posed for a continuous-time/ discrete-time model of the form of Eqs. 9 and 10, are covered in Table 1 of Ref. 11, as summarized on p. 278 and 338 of Ref. 8. This implementation differs from that of a standard Kalman filter for purely linear systems only in the Propagate and Update Steps of the filter (viz., compare the last row of Table 1 here with the last row of Table 1 in Ref. 13). Both implementations appear similar. However, an implicit difference is that $\Phi(k, k-1)$ is now a function of the measurements, z_k, since it is now to be obtained as a linearization about the estimate $\hat{x}_{k-1|k-1}$, which itself is a function of the measurement z_k. Consequently, the Propagate Step of the covariance $P_{k|k-1}$ in Table 1 is implicitly a function of z_k since $\Phi(k, k-1)$ *is* and so is the EKF filter gain K_k. A slight variation on the above EKF approach (as addressed in detail in Sec. 1.2 of Ref. 11) is to iterate within the linearization step a few times to greatly improve the quality of the estimates with but a slight penalty in increased number of operations.

Unlike what had been claimed [16], we recommend that the filter gain calculation be performed during the propagate step [11] since all its constituent components are already available during the propagate step. By performing this calculation within this step, the burden of what remains to be done during the (more time critical) update step is reduced. We amend Ref. 16 here as we have done on prior occasions [43], where two apparent errors existing in Ref. 16 are revealed pertaining to Kalman filter implementation by (1) exposing a flaw within a favored reduced-order MVRO filter formulation and (2) by correcting how the matrix pseudo-inverse should be calculated. Moreover, we have corrected a test for matrix positive semi-definiteness [46] that had persisted in error in more than a dozen textbooks (as listed in Ref. 46 and in its precursor references) and in most software implementations that we had seen in the 1970's and '80's for submarine navigation filters and for sonobuoy target tracking filters. We also offered a simplification [11] that corrects prior errors [16], [19], which otherwise inadvertently inflated the expected computational burden of an iterated EKF implementation beyond what is needed.

4. CRLB for Radar Target Tracking

[4] The EKF mechanization is to be distinguished from the so-designated *linearized Kalman filter* Table 6.1-3, p. 189 of Ref. 16, which is also applied to the linearized versions of the system and measurement equations of Eqs. 9 and 10, respectively, but for which filter gains can be precalculated, unlike the situation for an EKF.

4.1 Target Motion and Radar Sensor Models

Ref. 29 offers a good discussion of how to formulate the problem of radar tracking of targets in ballistic trajectories and provides a derivation of the particulars of the appropriate mathematical model from first principles, as well as providing an accounting and motivation for use of the various necessary coordinate systems. Other important analytic modeling considerations underlying a rigorous analysis are treated [24] regarding use of either a ground based or airborne radar for tracking. We used these earlier results as we selected a mathematical model to be used here (as in Ref. 11).

In this investigation, a Keplerian trajectory is introduced within a detailed simulation of the exoatmospheric target motion to include the effect of an inverse square pull of gravity. We refrain from just the use of simplified covariance analysis (essentially corresponding to evaluation of a Cramer-Rao lower bound for the estimation objective in the exoatmospheric regime of no process noise being present, as used in earlier investigations [26], [30]) and we instead now incorporate full nonlinear filtering techniques (and the associated standard approximations). Instead of linearizing about the true target, as done in prior simplified covariance analysis, the Extended Kalman Filter linearizes about the filter state estimates at each time-step. [5]

We work with a fully nonlinear 6-state system model, which in continuous-time is of the form:

$$\frac{d}{dt}\begin{bmatrix} x_1 \\ x_2 \\ x_3 \\ x_4 \\ x_5 \\ x_6 \end{bmatrix} = \begin{bmatrix} x_4 \\ x_5 \\ x_6 \\ \frac{-\mu\, x_1}{(\sqrt{x_1^2+x_2^2+x_3^2})^3} \\ \frac{-\mu\, x_2}{(\sqrt{x_1^2+x_2^2+x_3^2})^3} \\ \frac{-\mu\, x_3}{(\sqrt{x_1^2+x_2^2+x_3^2})^3} \end{bmatrix} \triangleq f(x)\,, \quad (11)$$

where μ is the familiar gravitational constant earth mass product GM. This is one of the equations that had to be linearized in implementing an Extended Kalman Filter and for which a Jacobian for the nonlinearity on the right hand side of Eq. 11 must be calculated.

Explicit evaluation of the requisite Jacobian, obtained by performing the indicated differentiations on the system nonlinearity $f(x)$, yields:

$$A(x) = \frac{\partial f(x)}{\partial x} = \begin{bmatrix} 0 & 0 & 0 & 1 & 0 & 0 \\ 0 & 0 & 0 & 0 & 1 & 0 \\ 0 & 0 & 0 & 0 & 0 & 1 \\ a_{41} & a_{42} & a_{43} & 0 & 0 & 0 \\ a_{51} & a_{52} & a_{53} & 0 & 0 & 0 \\ a_{61} & a_{62} & a_{63} & 0 & 0 & 0 \end{bmatrix}, \quad (12)$$

where the partial derivatives a_{ij} in the above were previously worked out [11], [42].

The resulting sensor measurements in terms of range, R, and the direction cosines, u and v, to the target are:

$$R = \sqrt{x'^2 + y'^2 + z'^2}, \quad (13)$$

$$u = \frac{x'}{R}, \quad (14)$$

$$v = \frac{y'}{R}, \quad (15)$$

where x', y', and z' are to be defined next.

The local coordinates x, y, z are located at the center of the sensor face in the plane of the array. In this coordinate system, z is directed along the local vertical and x and y lie in the horizontal plane, with x pointing East and y pointing North. From Sec. II of Ref. 29, these local level coordinates x, y, z can be reexpressed in terms of x', y', z' coordinates, via the following transformation

$$\begin{bmatrix} x' \\ y' \\ z' \end{bmatrix} = T \begin{bmatrix} x \\ y \\ z \end{bmatrix},$$

where

$$T = \begin{bmatrix} \cos\lambda & -\sin\lambda & 0 \\ \cos\phi\sin\lambda & \cos\phi\cos\lambda & -\sin\phi \\ \sin\phi\sin\lambda & \sin\phi\cos\lambda & \cos\phi \end{bmatrix},$$

as the appropriate change of coordinates corresponding to the required rotation, where the above parameters of λ and ϕ, are geodetic Latitude and Longitude, respectively. The coordinates x', y', z' are oriented so that z' is normal to the face of the sensor array, and y' lies on the face of the array, and x lies along the intersection of the sensor face and the horizontal plane [6].

[5] The target complex tracking problem is decomposed into primary and secondary contributing effects [19] to be considered in the modeling, and the effect of a rotating earth on the overall problem is of the later category.

[6] R. M. Miller's software implementation code for getting between sensor Face Centered Coordinates to Earth Centered Inertial coordinates [24] avoids sinusoids within

The above received sensor signal-processed measurement can be reexpressed in terms of the measurement of target range (as appropriate for a radar or other active sensor if not range-denied due to jamming), elevation, and azimuth as, respectively:

$$r = \sqrt{x^2+y^2+z^2}, \quad (16)$$

$$E = arctan\left[\frac{z}{\sqrt{x^2+y^2}}\right], \quad (17)$$

$$A = arctan\left[\frac{x}{y}\right], \quad (18)$$

where the length in Eq. 16 is identical to the length in Eq. 13 since the transformation T is a rotation (and as such is an orthogonal transformation which preserves lengths). The expressions of Eqs. 16 to 18 correspond to the following measurement equation:

$$z(t) = \begin{bmatrix} r \\ E \\ A \end{bmatrix} + v(t)$$

$$= \begin{bmatrix} \sqrt{x^2+y^2+z^2} \\ arctan\left[\frac{z}{\sqrt{x^2+y^2}}\right] \\ arctan\left[\frac{x}{y}\right] \end{bmatrix} + v(t), \quad (19)$$

where the Gaussian white measurement noise, $v(t)$, has a covariance that is of the form [7]

$$R = \begin{bmatrix} \sigma_r^2 & 0 & 0 \\ 0 & \sigma_E^2 & \\ 0 & 0 & \frac{\sigma_E^2}{cos^2(E)} \end{bmatrix}, \quad (20)$$

and the proper values to use for these variances are provided with our numerical results in Sec. 5.1.

An additional aspect not to overlook is that target location is referred back to ECI coordinates within the software by subtracting out the known location of the stationary radar array as an offset or translation. Notice that for the above described target complex motion model of Eqs. 11 and 19, respectively, both the system model *and* the measurement model are nonlinear. The linearization of the above nonlinear measurement of Eq. 19 is as provided on pp. 22, 23 of Ref. 24 and is a subset of that depicted and exhibited later [11], [42]. Operational implementations should additionally account for the flatness at the earth's poles as an oblate ellipsoid or sphere somewhat flattened at the poles and should include up to the J_2 gravity term, as discussed elsewhere [44].

The linearization of the current EKF is about the most recent state estimate $\hat{x}_{k|k}$ instead of the actual state (which is realistically presumed to be unknown to the observing sensor but is treated as known for CR lower bound evaluation via simulation here and could also accommodate evaluation using true position in trial flights using a GPS translator onboard the target).

4.2 Tailoring the CRLB Inequalities to Fit the NMD Target Tracking Scenario

The CRLB that is treated here goes beyond just using the historically familiar (pp. 155-161 of Ref. 17) per pulse CRLB angle measurement error [8]: $\sigma_\theta = \frac{\theta_3}{1.6\sqrt{2\ SNR}}$ since our CRLB goes further to additionally utilize **(1)** information provided by the target dynamics model over time in an inverse square gravity field, **(2)** the initial (starting) covariance $P(0)$ of the tracking filter as handed-over [9], and **(3)** the structure of the radar as a measurement sensor/device having additive Gaussian measurement noise with parameters including **(3a)** explicit use of the radar range uncertainty due to resolution size of the range gates and **(3b)** the monopulse SNR time-record with its adaptive step size (as a consequence of a realistically varying PRF) as it affects the corresponding angle uncertainty. In a more refined CRLB threat trajectory evaluation, we go further in seeking to use an input SNR that has been averaged over several Monte-Carlo trials ($\sim$ 5 or 10 trials but not averaged over time) to smooth out the telltale kinks due to noisy variations otherwise incurred within a single trial.

For our radar application, which has additive Gaussian white measurement noise $v(t)$, Eq. 2 has this further more benign and accommodating structure to be exploited:

$$z(t) = h(x,t) + v(t), \quad (21)$$

and since the equation for the system evolution is

the transformation by resorting instead to the underlying right triangles corresponding to each angle measurement. This alternative implementation appears to offer some nice efficiencies so we also employ it here in our investigation. There are standard approaches for transforming between Local Level and ECI coordinates [25].

[7] Within the software, we intentionally avoid the presence of the cosine in the denominator depicted in Eq. 20 by instead employing the following identity: $cos^2E = \frac{x^2+y^2}{x^2+y^2+z^2}$.

[8] Within this notation, θ_3 = 3 dB receive sum-pattern beamwidth.

[9] We used a standard hand-over covariance of (100 km)^2 for all three components of the position block and (100 m/sec)^2 for all three components of the velocity block.

essentially deterministic (with $Q_c = 0$ in Eq. 7), then the pdf's of interest here (to be used in numerically evaluating the CR lower bound of Eq. 1) are of the form:

$$p(z|x) = \frac{e^{-\frac{1}{2}(z-h(x))^T R^{-1}(z-h(x))}}{(2\pi)^{n/2}|R|^{-\frac{1}{2}}}. \quad (22)$$

Now taking natural logarithms on both sides of the above pdf yields:

$$\ln\{p(z|x)\} = -\frac{1}{2}(z-h(x))^T R^{-1}(z-h(x)) - \ln(2\pi)^{n/2}|R|^{-\frac{1}{2}}, \quad (23)$$

which upon taking the gradient is:

$$(\frac{\partial}{\partial x})^T \ln\{p(z|x)\} = \frac{\partial^T h(x)}{\partial x} R^{-1}(z-h(x)). \quad (24)$$

When the above expression is post-multiplied by its transpose and expectation taken throughout, the result is:

$$E[(\frac{\partial}{\partial x})^T \ln\{p(z|x)\} \frac{\partial}{\partial x} \ln\{p(z|x)\}] = \frac{\partial^T h(x)}{\partial x} R^{-1} \overbrace{E[(z-h(x))(z-h(x))^T]}^{R} R^{-1} \frac{\partial h(x)}{\partial x} = \frac{\partial^T h(x)}{\partial x} R^{-1} \frac{\partial h(x)}{\partial x}. \quad (25)$$

Finally, over corresponding discrete-time steps (not necessarily uniform), the total pdf of independent (white) measurements is the product of each individual pdf of the same form of Eq. 22 as $p(z_1|x(0))p(z_2|x(0))p(z_3|x(0))\cdots p(z_k|x(0))$, where each pdf for each constituent measurement here focuses on or is conditioned on the initial condition for the deterministic system equation. Once the initial condition $x(0)$ is known with confidence, then the time evolution of the deterministic system is completely determined (as a consequence of initial condition observability, as explained in App. A of Ref. 42). The corresponding information matrix for each of these measurement time points is of the form of Eq. 25 so the aggregate is of the form [10]:

$$\mathcal{I}(k,0) = \sum_{j=1}^{k} \Phi^{-T}(k,j) \frac{\partial^T h(x)}{\partial x}|_j R^{-1}(j,j) \frac{\partial h(x)}{\partial x}|_j \Phi^{-1}(k,j), \quad (26)$$

[10] After taking the natural logarithm of the aggregate pdf, the exponents in the Gaussian distribution correspond to the indicated sum, after performing a gradient and taking expectations, as illustrated in detail above in Eqs. 22 to 25 for just a single measurement for clarity.

for $k \geq j$, where the transition matrix $\Phi^{-1}(k,j) \triangleq [\Phi(k,j)]^{-1} = \Phi(j,k)$ and, likewise, corresponds to an evaluation via. Eq. 6 of the linearized system matrix $\frac{\partial f}{\partial x}|_j$, as previously explained [7].

Now, when there is a finite initial covariance being utilized by the estimator as tracking commences, then there is an additional term [11] that should appear in the above Information matrix to properly reflect this situation, as depicted as the first term on the RHS here:

$$\mathcal{I}(k,0) = \Phi^{-T}(k,0)P^{-1}(0)\Phi^{-1}(k,0) + \sum_{j=1}^{k} \Phi^{-T}(k,j) \frac{\partial^T h(x)}{\partial x}|_j R^{-1}(j,j) \frac{\partial h(x)}{\partial x}|_j \Phi^{-1}(k,j). \quad (27)$$

In either the case of Eq. 26 or Eq. 27 holding, the Information matrix can be interpreted or formulated as evolving recursively with each received measurement arrival time (with either a constant or varying time-step) as:

$$\mathcal{I}(k,0) = \Phi^{-T}(k,j)\mathcal{I}(j,0)\Phi^{-1}(k,j) + \frac{\partial^T h(x)}{\partial x}|_k R^{-1}(k,k) \frac{\partial h(x)}{\partial x}|_k \quad (28)$$

and, as such, may be implemented within software as merely a loop (but by observing all the constraints and coordinate conventions of Sec. 4.1, where $\frac{\partial f}{\partial x}$ is evaluated within the ECI frame and $\frac{\partial h}{\partial x}$ is evaluated in the (E,N,U) frame with corresponding translation offset to the location of the tracking radar) [12]. The computational burden or operations counts per cycle of such a software implementation goes as n^3 due to the three fundamental $n \times n$ matrix multiplies present and also scales linearly with the number of time steps included.

[11] An additional "fictitious measurement" was called for following Eq. 4 of Ref. 7 as being needed to avoid encountering numerical difficulties but use of $P^{-1}(0)$ as suggested here appears to suffice as a remedy that arises naturally.

[12] Notice that nothing was presumed of the estimator in deriving and evaluating Eq. 28 beyond the underlying measurement structure of Eqs. 21, 22 and the availability of all measurements up to the current time k. Alternative estimators that "smooth" by estimating the state x_k using measurements beyond k may violate this assumption and this CRLB but they aren't real-time and thus not usually of interest in this application. The appropriate CRLB to correspond to an estimator that uses measurements beyond the current time of interest (such as in "sliding window" smoothing or in "fixed point" smoothing or in "batch least squares or maximum likelihood") should just have the additional corresponding terms included in Eqs. 26 and 27 and could still be mechanized via an appropriately modified Eq. 28.

We have particular interest in the total position error and the corresponding total velocity error to determine how well we are actually doing in tracking a target complex via radar. To this end, we must rigorously contort the inequality of Eq. 1 to a form that we can use. This is accomplished by properly applying matrix operations that preserve the ordering yet eventually yield the expressions that we seek [13] as, first:

$$\begin{bmatrix} \sigma_{11}^2 & \sigma_{12}^2 & \sigma_{13}^2 \\ \sigma_{21}^2 & \sigma_{22}^2 & \sigma_{23}^2 \\ \sigma_{31}^2 & \sigma_{32}^2 & \sigma_{33}^2 \end{bmatrix} =$$

$$\begin{bmatrix} 1 & 0 & 0 & 0 & 0 & 0 \\ 0 & 1 & 0 & 0 & 0 & 0 \\ 0 & 0 & 1 & 0 & 0 & 0 \end{bmatrix} E[(x_{true}(t) - \hat{x}(t))(x_{true}(t) - \hat{x}(t))^T | \mathcal{Z}(t)] \begin{bmatrix} 1 & 0 & 0 & 0 & 0 & 0 \\ 0 & 1 & 0 & 0 & 0 & 0 \\ 0 & 0 & 1 & 0 & 0 & 0 \end{bmatrix}^T \geq \tag{29}$$

$$\begin{bmatrix} 1 & 0 & 0 & 0 & 0 & 0 \\ 0 & 1 & 0 & 0 & 0 & 0 \\ 0 & 0 & 1 & 0 & 0 & 0 \end{bmatrix} \mathcal{I}^{-1} \begin{bmatrix} 1 & 0 & 0 & 0 & 0 & 0 \\ 0 & 1 & 0 & 0 & 0 & 0 \\ 0 & 0 & 1 & 0 & 0 & 0 \end{bmatrix}^T = \begin{bmatrix} crlb_{11} & crlb_{12} & crlb_{13} \\ crlb_{21} & crlb_{22} & crlb_{23} \\ crlb_{31} & crlb_{32} & crlb_{33} \end{bmatrix}$$

and

$$\begin{bmatrix} \sigma_{44}^2 & \sigma_{45}^2 & \sigma_{46}^2 \\ \sigma_{54}^2 & \sigma_{55}^2 & \sigma_{56}^2 \\ \sigma_{64}^2 & \sigma_{65}^2 & \sigma_{66}^2 \end{bmatrix} =$$

$$\begin{bmatrix} 0 & 0 & 0 & 1 & 0 & 0 \\ 0 & 0 & 0 & 0 & 1 & 0 \\ 0 & 0 & 0 & 0 & 0 & 1 \end{bmatrix} E[(x_{true}(t) - \hat{x}(t))(x_{true}(t) - \hat{x}(t))^T | \mathcal{Z}(t)] \begin{bmatrix} 0 & 0 & 0 & 1 & 0 & 0 \\ 0 & 0 & 0 & 0 & 1 & 0 \\ 0 & 0 & 0 & 0 & 0 & 1 \end{bmatrix}^T \geq \tag{30}$$

$$\begin{bmatrix} 0 & 0 & 0 & 1 & 0 & 0 \\ 0 & 0 & 0 & 0 & 1 & 0 \\ 0 & 0 & 0 & 0 & 0 & 1 \end{bmatrix} \mathcal{I}^{-1} \begin{bmatrix} 0 & 0 & 0 & 1 & 0 & 0 \\ 0 & 0 & 0 & 0 & 1 & 0 \\ 0 & 0 & 0 & 0 & 0 & 1 \end{bmatrix}^T = \begin{bmatrix} crlb_{44} & crlb_{45} & crlb_{46} \\ crlb_{54} & crlb_{55} & crlb_{56} \\ crlb_{64} & crlb_{65} & crlb_{66} \end{bmatrix},$$

and then by taking the trace of a matrix throughout [14], respectively, yields **radial position error variance**:

$$\begin{aligned} \sigma_{position}^2 = \sigma_{11}^2 + \sigma_{22}^2 + \sigma_{33}^2 \quad &= \quad \textbf{trace} \begin{bmatrix} \sigma_{11}^2 & \sigma_{12}^2 & \sigma_{13}^2 \\ \sigma_{21}^2 & \sigma_{22}^2 & \sigma_{23}^2 \\ \sigma_{31}^2 & \sigma_{32}^2 & \sigma_{33}^2 \end{bmatrix} \geq \\ \textbf{trace} \begin{bmatrix} crlb_{11} & crlb_{12} & crlb_{13} \\ crlb_{21} & crlb_{22} & crlb_{23} \\ crlb_{31} & crlb_{32} & crlb_{33} \end{bmatrix} \quad &= \quad crlb_{11} + crlb_{22} + crlb_{33} \end{aligned} \tag{31}$$

and **total velocity error variance**:

$$\begin{aligned} \sigma_{velocity}^2 = \sigma_{44}^2 + \sigma_{55}^2 + \sigma_{66}^2 \quad &= \quad \textbf{trace} \begin{bmatrix} \sigma_{44}^2 & \sigma_{45}^2 & \sigma_{46}^2 \\ \sigma_{54}^2 & \sigma_{55}^2 & \sigma_{56}^2 \\ \sigma_{64}^2 & \sigma_{65}^2 & \sigma_{66}^2 \end{bmatrix} \geq \\ \textbf{trace} \begin{bmatrix} crlb_{44} & crlb_{45} & crlb_{46} \\ crlb_{54} & crlb_{55} & crlb_{56} \\ crlb_{64} & crlb_{65} & crlb_{66} \end{bmatrix} \quad &= \quad crlb_{44} + crlb_{55} + crlb_{66}, \end{aligned} \tag{32}$$

and, finally, by taking squareroots throughout [15], respectively, yields:

$$\sigma_{position} = \sqrt{\sigma_{11}^2 + \sigma_{22}^2 + \sigma_{33}^2} \geq \sqrt{crlb_{11} + crlb_{22} + crlb_{33}} \triangleq \text{CRLB}_{position} \tag{33}$$

and

$$\sigma_{velocity} = \sqrt{\sigma_{44}^2 + \sigma_{55}^2 + \sigma_{66}^2} \geq \sqrt{crlb_{44} + crlb_{55} + crlb_{66}} \triangleq \text{CRLB}_{velocity}. \tag{34}$$

[13] Pre- and post-multiplying $A \geq B$ by the same matrix L yields $LAL^T \geq LBL^T$.

[14] The matrix inequality $A \geq B$ implies that trace$[A] \geq$ trace$[B]$.

[15] Scalar $a \geq b \geq 0$ implies that $\sqrt{a} \geq \sqrt{b}$.

Please notice in the above that we do not decouple position and velocity states but merely project both of the 6 × 6 matrices of Eq. 1, respectively, into the position subspace (as Eqs. 29, 31, 33) and into the velocity subspace (as Eqs. 30, 32, 34) for viewing and display. These instantaneous inequalities are now the theoretically justified comparisons that we invoke again in Sec. 5.1 in monitoring EKF target tracking performance as a function of time.

5. Assessing EKF Tracking Performance

5.1 BASELINE: Comparing Existing Standard EKF to the Computed CRLB

We illustrate the CRLB calculations relative to ensemble sampled Monte-Carlo results for the BMEWS radar: Thule [16] tracking an RV on a ballistic trajectory (post cut-off) having the following position and velocity states at cut-off time normalized to $t_o = 0$ secs.:

$$\begin{bmatrix} x(t_0) \\ y(t_0) \\ z(t_0) \\ v_x(t_0) \\ v_y(t_0) \\ v_z(t_0) \end{bmatrix} = \begin{bmatrix} -3217302.678 \\ 3527834.349 \\ 4535013.695 \\ -767.670 \\ -2520.638 \\ 5065.414 \end{bmatrix}, \quad (35)$$

where in the above, the units are in meters for position and meters/sec for velocity, respectively.

The simulations of the radar case [using known BMEWS measurement covariances for range and angle being [17]

$$\begin{aligned} \sigma_{range} &= 30 \text{ meters (per pulse)}, \\ \sigma_{angle} &= \frac{2.2}{1.6\sqrt{2\,\mathrm{SNR}}} \text{ degrees (per pulse)}, \end{aligned} \quad (36)$$

respectively] [18] appear to be performing properly as depicted in Fig. 1 for the case of a nonlinear target (corresponding to use of the system model of Eq. 11 for simulating the trajectory, but linearized within the EKF) while both situations utilized the nonlinear measurement model of Eq. 19. Both parameters in Eq. 36 (with SNR varying with time) are used in Eq. 20 with $\sigma_E \equiv \sigma_{angle}$.

For position error at time t (and similarly for corresponding velocity with obvious direct replacement substitutions of velovities for positions in Eqs. 37 and 38 below), calculated as

$$\sqrt{(x_{true}(t) - \hat{x}(t))^2 + (y_{true}(t) - \hat{y}(t))^2 + (z_{true}(t) - \hat{z}(t))^2}, \quad (37)$$

the corresponding sampled variance over N trials ($N = 1,000$) being [19]:

$$\Sigma_N = \left[\frac{1}{N}\sum_{i=1}^{N}(x_{true}(t) - \hat{x}_i(t))^2 + (y_{true}(t) - \hat{y}_i(t))^2 + (z_{true}(t) - \hat{z}_i(t))^2\right] - \left[\frac{1}{N}\sum_{i=1}^{N}\sqrt{(x_{true}(t) - \hat{x}_i(t))^2 + (y_{true}(t) - \hat{y}_i(t))^2 + (z_{true}(t) - \hat{z}_i(t))^2}\right]^2, \quad (38)$$

is depicted here as labeled while the CRLB is shown in juxtaposition as labeled in Figs. 1 and 2 for total position error and total velocity error, respectively, in tracking an RV (Scenario D10.4). While in the early stages of the first few initial time steps in Fig. 1, there can be a slight discrepancy of the averaged sampled standard deviation dipping down below the CRLB (which should be a theoretical impossibility), it occurs here only briefly at the beginning because there is an initialization procedure being applied only to the EKF in obtaining the starting $\hat{x}(0)$ (that is subsequently linearized about in the EKF). The general trend is that the calculated CRLB is below the error of the EKF (as it should be theoretically for this and all standard state estimators) but the EKF appears to asymptotically approximate it pretty well (note that this is a semi-logarithmic scale that tends to compress differences). The lowest curve appearing in Figs. 3 and 4 conveys another aspect of the story as the EKF's internally calculated [20] single shot estimate of its own standard deviation (also labeled). This single shot self assessment of standard deviation for nonlinear estimators is known to usually be unreliable, not just in this application but in any nonlinear situation (e.g., Sec. 8.12 of Ref. 8, Fig. 2 of Ref. 39) but is depicted nonetheless to convey just how far off it is, in general, from what is actually present (as established

[16] This 10 MHz bandwidth Thule radar (AN/FPS-123V5), with a beamwidth of 1.8° is located in Greenland at Latitude = 76.56° N, Longitude = 297.70° E. The actual range resolution is determined by beam forming to reduce sidelobes and assumptions on range accuracy of from as little as 15 meters (for the 10 MHz signal) up to more than 30 meters (for the 5 MHz signal) shouldn't significantly alter the subsequently computed results since sensitivity to the range uncertainty parameter is low as compared to the effect of the more dominant angle uncertainty.

[17] Expressed within our software in MKS units with angles in radians, respectively.

[18] The radar's intrinsic range gate size dictates the effective range resolution, which is a constraint that is less restrictive than the angle acuity. The expression for σ_{angle} is identical to what appears in the first sentence in Sec. 4.2.

[19] Notice that this is of the form $E[(W - E[W])^2] = E[W^2] - (E[W])^2$.

[20] Calculated via a matrix Riccati differential equation or recursive difference equation, which for nonlinear applications is an explicit function of the measurement values received and is merely an approximate representation, while for linear applications it would be exact.

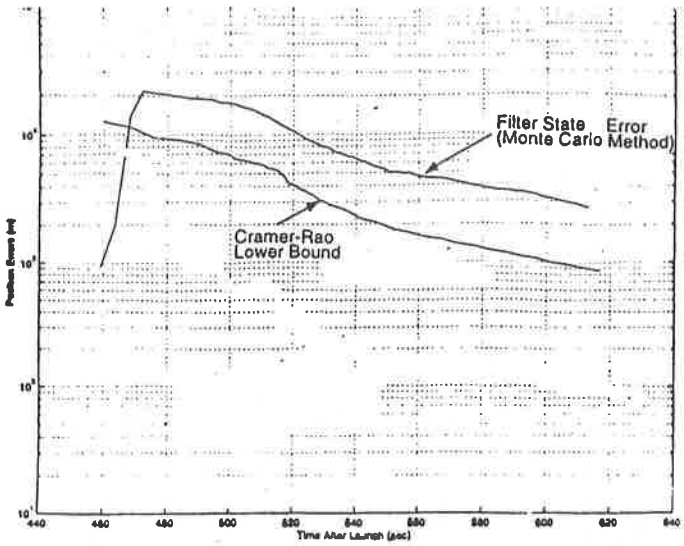

Figure 1: Results Comparing EKF Performance (Sampled Standard Deviation, $N = 1000$) and Comparable CRLB in Tracking of an RV's Position vs. Time

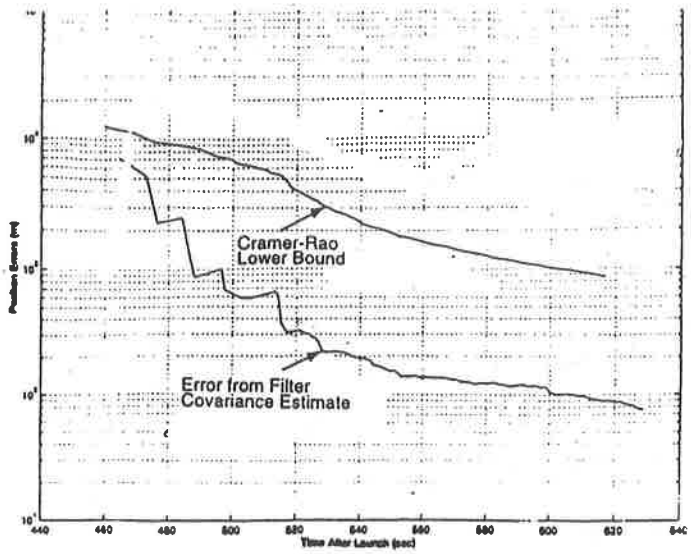

Figure 3: Results Comparing EKF Self Assessment of Performance (from Ricatti Eq., $N = 1$) and Comparable CRLB in Tracking of a Tank's Position vs. Time

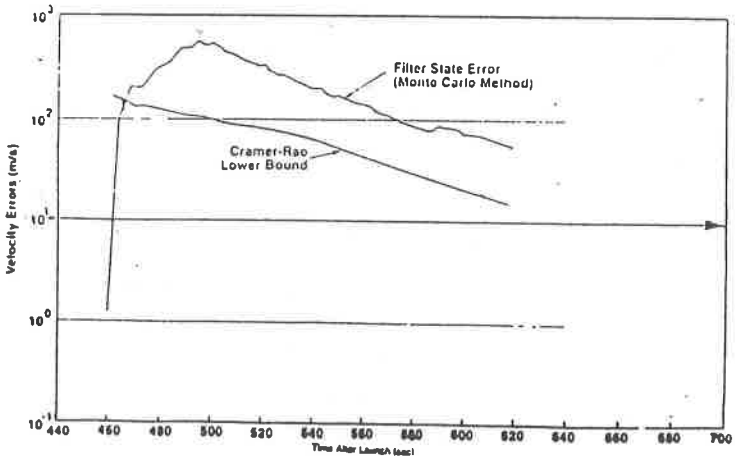

Figure 2: Results Comparing EKF Performance (Sampled Standard Deviation, $N = 1000$) and comparable CRLB in Tracking of an RV's Velocity vs. Time

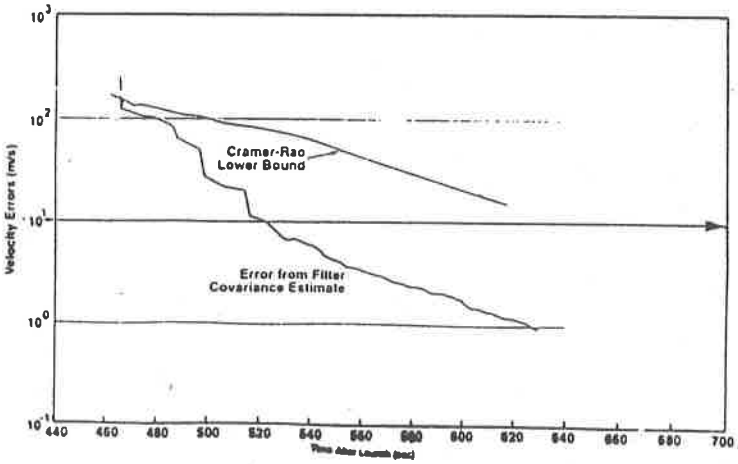

Figure 4: Results Comparing EKF Self Assessment of Performance (from Ricatti Eq., $N = 1$) and comparable CRLB in Tracking of a Tank's Velocity vs. Time

by the large number: 1000 of Monte Carlo trials). It is only this estimator's Riccati calculated standard deviation that is **actually available during a mission** also as a single shot $N = 1$. Perhaps other alternative estimators will be more reliable (by having single shot covariances that are closer to the ideal CRLB or acceptable sample average standard deviation) and should be further sought out in a more detailed investigation of trackers for NMD.

Figs. 1 and 2, discussed above, representatively illustrate calculated CRLBs and other components, listed at the beginning of Sec. 4, used in comparing RV tracking performance (for Scenario D10.4, with coded launch point and threat characteristics and target as defined in System Requirements Document C1= Capability One). Figs. 3 and 4 representatively illustrate calculated CRLBs and other components used in comparing tank tracking performance (for Scenario D10.5).

Please notice from Figs. only shown in [42] that (at this scale) the Monte-Carlo statistics of EKF performance at high SNR are close to the ideal CRLB. This indicates that EKF performance is fairly good in the tank tracking role as one of the primary goals for Updated Early Warning Radar UEWR (of successfully detecting, tracking, and handing over the location of tanks) and so can the narrow-field-of-view X-band radar that is also directed to perform further search in the same vicinity. Using the presence of tanks as its cue, the UEWR radar can then search for other threatening objects nearby. Please notice from Figs. 1 and 2 that the Monte-Carlo statistics of EKF tracking performance for the RV are not as correspondingly close to the ideal CRLB (as they had been for the tank). This indicates that there is room for improvement in estimator tracking performance (where such improvements are currently being actively sought along different novel development paths by several participating NMD contractors and MITRE) with additional novel options [11], [18], [38]– [40], [45] yet to be explored for NMD.

While the CRLB software implementation originally assumed measurements and associated SNR to be available at a constant 1 Hz rate, the CRLB software was later modified to adaptively handle SNR at a variable rate whenever it became available as a consequence of the radar resource "scheduler", initialization, threshold setting [21], and other internal signal processing. One example of further internal signal processing is the performing of coherent integration (in summing returns and keeping track of phase as in-phase and quadrature phase) in PP and OP returns treated as real and imaginary parts, respectively, of the received signal as a phasor. This is used to detect and track those targets exhibiting smaller relative radar cross-sections. In all cases, the CRLB software just uses the resultant SNR time record to calculate the bound. The TD/SAT Monte-Carlo simulator outputs the SNR that CRLB calculations use as input. In order to remedy the jagged edges that sometimes occur in a single SNR time record, we usually seek to average the results from a modest 5 to 10 Monte-Carlo trials to get a resultant SNR input that is slightly smoother and more universally representative so that computed CRLB output is likewise more universal and not tied to just a single Monte-Carlo run.

Fig. 5 depicts the sample average or Mean Estimation Error vs. Time as arises in the RHS of Eq. 38 (for Scenario D10.4), which differs, in general, from the standard deviations of Fig.1. The CRLBs are appropriate for comparison only to Standard deviations (as in Eq. 23) or to variances (as in Eq. 21). This mean or bias in the estimator represents a type of Kentucky windage [22] (that potentially can be calibrated and compensated for each target tracking filter on a trajectory by trajectory basis) as is well-known to occur in SLBM's as well.

While only one representative trajectory is depicted here to illustrate the CRLB evaluation technique and to show what type of comparisons we used between CRLB and sampled estimator statistics in the standard deviation domain, TeK Associates implemented the software and performed the evaluations for more than 50+ different trajectories (also from the perspective of various alternative radar in view) during the course of this investigation. We would expect the new optimal estimator [45] to perform better than the simple but straightforward EKF displayed here.

5.2 Refinements/Extensions to Our Current CRLB

We make the following suggestion regarding how to further refine the information provided by the CRLB in a manner to better quantify the "fly-out" situation where kinetic kill vehicles would be dispatched via *command guidance* to intercept and destroy an RV after it is detected and recognized as a threat by the strategic radar fence.

[21] The detection threshold is nominally 11.5 (unitless) corresponding to a per pulse false alarm rate of 10^{-6}.

[22] Gunnery terminolgy that harkens back to Sgt. Alvin York's remarkable feats of marksmanship during WWI in compensating for the bias of a cross-wind.

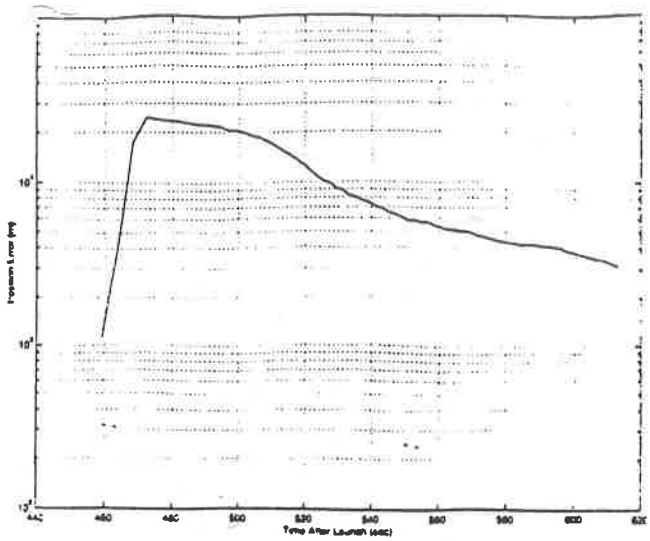

Figure 5: Results Comparing EKF Performance (Sampled Mean Error, $N = 1000$) in Tracking of an Object's Position vs. Time

Such information and interpretation would be useful in providing weapon system specifications for the missile and analysis of its perceived effectiveness. Using the following notation,

$$T_f = \text{kinetic kill vehicle intercept time of traverse,} \tag{39}$$

then [23]

$$\begin{aligned}
&\text{Missile Dispatch Position Error Variance}(k) \\
&= [\text{Projected Position Error(from } k \text{ to } k+T_f)] \\
&= \mathbf{trace}\left\{ [I|0]\Phi^{-T}(k+T_f,k)\Sigma(k,0)\Phi^{-1}(k+T_f,k)]^{-1} \begin{bmatrix} I \\ \cdots \\ 0 \end{bmatrix} \right\} \\
&= \mathbf{trace}\left\{ [I|0]\Phi(k+T_f,k)\Sigma^{-1}(k,0)\Phi^{T}(k+T_f,k)] \begin{bmatrix} I \\ \cdots \\ 0 \end{bmatrix} \right\},
\end{aligned} \tag{40}$$

which can be calculated and plotted for each time point k for a total elucidation after taking the squareroot of both sides to yield a standard deviation. This would still be a function of each trajectory and radar location and corresponding parameters of the viewing radar.

[23] **Caveat:** Although the representative expression for the transition matrix appearing in Eq. 40 could be incorrectly interpreted as needing to be calculated only once; as a practical matter, it should be calculated incrementally ($\sim$ 1 Hz) as $\Phi(k+T_f,k) = \Phi(k+T_f,j_s)\Phi(j_s,j_{s-1})\Phi(j_{s-1},j_{s-2})\cdots\Phi(j_2,j_1)\Phi(j_1,k)$ where $k+T_f > j_s > j_{s-1} > \cdots > j_1 > k$ within the software mechanization (via Eqs. 6 and 12, where $F \equiv A$) in order to adequately correspond to the solution of Eq. 11, which is nonlinear.

In evaluating the 0.97 Spherical Error Probable (SEP) for each trajectory, one can use the estimated sample covariances from several Monte-Carlo trials for a particular estimator and compare to what is obtained from one run of the CRLB. The behavior of the computed CRLB will exhibit the expected ellipsoidal shape of first being pan-cake shaped at the begining owing to the radar resolution uncertainty that is relatively less in the range direction and greater in the angular directions of elevation and azimuth and, as time elapses, becoming more football shaped later with a principal axis in the direction of the instantaneous velocity. The vertical velocity of the target at zenith in a ballistic trajectory is of course zero.

Rather than calculate 0.97 SEP, an easier calculation is to use a bounding ellipsoid that exactly matches the underlying Gaussian sufaces of constant pdf as they vary with time. In this way, the results for a tailored time-varying 3-D ellipsoid having 0.97 probability of containing the target under an assumed underlying Gaussian distribution can be read from existing tabulations of Chi-square statistics with 3 degrees-of-freedom (dof) that remain constant with time (analytic details for accomplishing this are on pp. 106-7 of Ref. 41). Even if there is a quantifiable bias present, the offset effect is accounted for by instead using well tabulated non-central Chi-squared statistics of 3 dof rather than attempt SEP calculations which are more challenging. Acknowledging that down-stream missile intercept divert capability re-

lates to the amount of available fuel onboard and is consequently reflected as a sphere of reachable positions; even so, the 3-D ellipsoids can be circumscribed by a 3-D sphere as a second calculation (for a total of two easy calculations rather than one harder SEP calculation) to appropriately match-up with what's needed.

6. Summary and Recommendations

We observed good agreement between the sampled standard deviations and the CRLBs that were implemented (consistent with the existing supporting theory that anticipates CRLB's to always fall below sample variances calculated from trials that are large enough to be significantly close to actual true values). The EKF's own internal assessment was NOT consistent with the CRLB, also as anticipated (and consistent with existing theory [39]) since these EKF covariances are only approximate in nonlinear applications such as this and, as such, are not always expected to be consistent and trustworthy (while in a linear application they would be trustworthy and, moreover, would represent the target goal to which Monte-Carlo statistical evaluations should be compared). Since it is the on-line estimator's standard deviation or variance that is used in calculating on-line gains that ultimately determine the accuracy of actual on-line estimates of target location and velocity within the mission (where, effectively, $N = 1$), considerations (in comparison to CRLB's as offered here) of having good reliable standard deviations within a mission is a goal that is necessary for adequate target tracking. Sampled standard deviation error discrepancies must be small in order for the associated estimation errors to be small. This conclusion is a consequence of the fact that the filter's actual covariances are to be calculated on-line from measurements received in only one time record. These single-shot covariances are used in the actual filter implementation on-line to calculate the filter gains that in turn determine what single-shot estimates of target position and velocity are ultimately produced (as conveyed to the kinetic kill vehicle that is dispatched to intercept and dispose of the target threat).

Suggested follow-on activities for further use of CRLB evaluations in strategic missile defense to an advantage are: **(1)** pursuing the following interesting and relevant philosophical alternative of seeking to perform target tracking using a system model that is posed in radar face coordinates just as the measurement equation currently is in Eq. 3.26 of Ref. 42. With such a recasting, the received measurements would indeed be a linear function of the states (as the parameter that is being sought), so the corresponding new CRLB would be *tight* according to the conditions previously laid out [6], [3] indicating that, at each timestep, the sampled error variance would then be expected to actually achieve or match the alternative CRLB [24] that corresponds to this hypothesized reformulated system state equation; **(2)** to develop a CRLB methodology for endoatmospheric targets since new rigorous results are now available [10], [31], [32] for handling CRLB evaluations for the case of a non-zero process noise covariance Q; **(3)** using the CRLB formulation for non-zero process noise to gauge the effect of alternative weightings in filter tuning exercises; **(4)** to develop a CRLB methodology for angle-only tracking scenarios [35] (to handle the case corresponding to jammers being present amongst the incoming target complex that can deny a surveillance radar's target tracking range determination); **(5)** to develop a CRLB methodology for satellite-borne down looking terrestrial applications experiencing backscatter from land clutter, sea clutter, and clouds using fairly recent evaluation techniques [47]. IR Images can also be handled [48].

A. Both CRLB and Filter Behavior Critically Depend on Actual Measurement Noise Covariance Evolution (as ultimately affects SNR)

The following closed-form solution from p. 126 of Ref. 16 (corresponding to a linear Kalman filter for a constant coefficient linear system) only considers an easy scalar case example. Consequently, all required manipulations are tractable and cause-effect results and relationships are revealed in a straight forward manner without being obscurred by complexity. Despite being merely a scalar example, it is still representative of all estimation problems involving Kalman filters or Kalman-like filters (such as an EKF) and it serves to reveal general trends and crutial dependencies and to also allow asymptotic steady-state behavior to be easily exhibited and deciphered. To this end, consider

[24] However, it's possible that the resulting CRLB arising for the alternative formulation proposed will likely be worse (larger than that associated with the current target model) since the current target model was in fact historically settled upon after other alternative formulations (e.g., [21], [22]) were explored and experimented with for this same strategic defense application scenario but which did NOT previously take into account the associated CRLB.

the following scalar system of the form of Eqs. 4 and 5 with underlying system matrix being zero ($f = 0$) and $g = h = 1$, and with scalar white, Gaussian process noise $w \sim \mathcal{N}(0, q)$ and scalar white Gaussian measurement noise $v \sim \mathcal{N}(0, r)$, respectively. The associated Riccati equation of Eq. 8 simplifies to be merely the following scalar differential equation:

$$\dot{p} = q - \frac{p^2}{r}, \text{ with specified initial condition : } p(o) = p_o. \tag{41}$$

Unlike the situation in the general case of interest, this scalar Riccati equation can be immediately solved by rearranging and employing the following identity:

$$\int \frac{dp}{\alpha^2 - p^2} = \frac{1}{\alpha} \ln \left[\frac{\alpha + p}{\alpha - p} \right], \tag{42}$$

and we find directly for $\alpha \triangleq \sqrt{rq}$ and $\beta \triangleq \sqrt{\frac{q}{r}}$ that the closed-form solution to the Riccati equation of Eq. 41 is:

$$p(t) = \alpha \left[\frac{p_o \cosh\{\beta\, t\} + \alpha \sinh\{\beta\, t\}}{p_o \sinh\{\beta\, t\} + \alpha \cosh\{\beta\, t\}} \right]. \tag{43}$$

Notice that a large initial uncertainty in this scalar Kalman filter-based tracking system would correspond to use of a relatively large initial uncertainty p_o and the above general solution involving the left most dominant terms in both numerator and denominator (where p_o divides out) reduces to:

$$p(t) = \alpha \coth\{\beta\, t\}. \tag{44}$$

Notice that within the above Eq. 44, the effective time constant is $\frac{1}{\beta} = \sqrt{\frac{r}{q}}$, so the rate of convergence dictated by the time constant is faster when the time constant is shorter, or for fixed q, when r is smaller. Since SNR appears in the denominator of the expression occurring within the first sentence of Sec. 4.2, having a larger SNR forces the associated r to be smaller and Eq. 44 converges faster. Notice further that the steady-state value as time gets large is $p(t) \to \alpha \equiv \sqrt{rq}$, and that this steady-state final value is smaller (corresponding to less uncertainty) when r is smaller too. Thus, there is a double benefit to having a large SNR to ensure a smaller r to achieve the most desirable outcome. As mentioned in Sec. 5.1, this double effect is why just approximating by using the average value of SNR in evaluating the CRLB of Eq. 28 should be avoided in favor of using the true instantaneous SNR values as a function of time to better reflect the underlying situation that exists.

Acknowledgments: The utility of results obtained by applying the Cramer-Rao Lower Bound (CRLB) evaluation methodology is depicted here in juxtaposition with outputs from the Extended Kalman Filter (EKF). We thankfully acknowledge that these EKF results were generated by Erik Slivka (MITRE) using the Test Driver (TD) and Software Algorithm Testbed (SAT), known collectively as TD/SAT. The SNRs that we used as inputs to the CRLB software were supplied by Erik Slivka and Chris Costner (MITRE) from TD/SAT. We also thankfully acknowledge guidance from Jim Pennington (MITRE).

REFERENCES

[1] Kerr, T. H., "A New Multivariate Cramer-Rao Inequality for Parameter Estimation (Application: input probing function specification," *Proceedings of IEEE Conference on Decision and Control*, Phoenix Az, pp. 97-103, 20-22 Nov. 1974.

[2] Nahi, N. E., *Estimation Theory and Applications*, Wiley, NY, 1969.

[3] Kerr, T. H., "Status of CR-Like Lower Bounds for Nonlinear Filtering," *IEEE Transactions on Aerospace and Electronic Systems*, Vol. 25, No. 5, pp. 590-601, Sept. 1989 (Author's reply in Vol. 26, No. 5, pp. 896-898, Sept. 1990).

[4] Rife, D. C., Goldstein, M., Boorstyn, R. R., "A Unification of Cramer-Rao Type Bounds," *Annals of Mathematical Statistics*, Vol. 30, No. 2, pp. 381-388, 1959.

[5] Weiss, A. J., Weinstein, E., "A Lower Bound on the Mean-Square Error in Random Parameter Estimation," *IEEE Trans. on Information Theory*, Vol. 31, No. 5, pp. 680-682, 1985.

[6] Fend, A. V., "On the Attainment of Cramer-Rao and Bhattacharyya Bounds for the Variance of an Estimate," *Annals of Mathematical Statistics*, Vol. 30, No. 2, pp. 381-388, 1959.

[7] Taylor, J. H., "Cramer-Rao Estimation Error Bound Analysis for Nonlinear Systems," *IEEE Transactions on Automatic Control*, Vol. 24, No. 2, pp. 343-345, April 1979.

[8] Jazwinski, A. H., *Stochastic Processes and Filtering Theory*, Academic Press,.N.Y., 1970.

[9] Maybeck, P. S., *Stochastic Models, Estimation, and Control*, Vol. 2, Academic Press, N.Y., 1982.

[10] Balakrishnan, A. V., *Kalman Filtering Theory*, Optimization Software, Inc., NY, Publications Division, 1987.

[11] Kerr, T. H., "Streamlining Measurement Iteration for EKF Target Tracking," *IEEE Transactions on Aerospace and Electronic Systems*, Vol. 27, No. 2, pp. 408-420, March 1991 (minor correction appears in Nov. 1991 issue).

[12] Van Trees, H. L., *Detection, Estimation, and Modulation Theory*, Part I, Wiley, NY, 1968.

[13] Kerr, T. H., "A Constructive Use of Idempotent Matrices to Validate Linear Systems Analysis Software," *IEEE Trans. on Aerospace and Electronic Systems*, Vol. 26, No. 6, pp. 935-952, Nov. 1990 (minor correction in Nov. 1991; Apr. 1995).

[14] Kerr, T. H., "Numerical Approximations and Other Structural Issues in Practical Implementations of Kalman Filtering," in *Approximate Kalman Filtering*, Guanrong Chen (ed.), pp. 193-220, World Scientific, Singapore, 1993.

[15] Kerr, T. H., and Satz, H. S., "Application of Some Explicit Formulas for the Matrix Exponential in Linear System Software Validation," *Proceedings of 16th Digital Avionics System Conference*, Irvine, CA, pp. 1.4-9 to 1.4-20, 25-30 October 1997.
[16] Gelb, A., Ed., *Applied Optimal Estimation*, MIT Press, Cambridge, MA, 1974.
[17] Berkowitz, R. S., *Modern Radar: analysis, evaluation, and system design*, John Wiley & Sons, NY, 1965.
[18] Gura, I. A., "Extension of Linear Estimation Techniques to Nonlinear Problems," *The Journal of Astronautical Sciences*, Vol. XV, No. 4, pp. 194-205, July/August 1968.
[19] Wishner, R. P., Larson, R. E., and Athans, M., "Status of Radar Tracking Algorithms," *Proceedings of Symposium on Nonlinear Estimation Theory and Its Applications*, San Diego, CA, pp. 32-54, 1970.
[20] Denham, W. F., and Pines, S., "Sequential Estimation When Measurement Function Nonlinearity is Comparable to Measurement Error," *AIAA Journal*, Vol. 4, pp. 1971-1076, 1966.
[21] Fitzgerald, R. J., "On Reentry Vehicle Tracking in Various Coordinate Systems," *IEEE Transactions on Automatic Control*, Vol. AC-19, No. 5, pp. 581-582, July 1974.
[22] Daum, F. E. and Fitzgerald, R. J., "Decoupled Kalman Filters for Phased Array Radar Tracking," *IEEE Transactions on Automatic Control*, Vol. AC-28, No. 3, pp. 269-283, March 1983.
[23] Kerr, T. H., "A Critical Perspective on Some Aspects of GPS Development and Use," *Proceedings of 16th Digital Avionics System Conference*, Irvine, CA, 25-30 October 1997 (a shorter version appears in Proceedings of St. Petersburg Navigation Conference, April 1997).
[24] Miller, R. W., and Chang, C. B., "Some Analytical Methods for Tracking, Prediction, and Interception Performance," Lincoln Laboratory Project Report No. RMP-129, Lexington, MA, 9 August 1977.
[25] Nash, R. A., Jr., Levine, S. A., and Roy, K. J., "Error Analysis of Space-Stable Inertial Navigation Systems," *IEEE Transactions on Aerospace and Electronic Systems*, Vol. AES-7, No. 4, pp. 617-629, July 1971.
[26] Miller, R. W., and Chang, C. B., "A Modified Cramer-Rao Bound and Its Applications," *IEEE Transactions on Information Theory*, Vol. IT-24, No. 3, pp. 398-400, May 1978.
[27] Chang, C. B., "Ballistic Trajectory Estimation with Angle-Only Measurements," *IEEE Transactions on Automatic Control*, Vol. AC-25, No. 3, pp. 474-480, June 1980.
[28] Bate, R. R., Mueller, D. D., White, J. E., *Fundamentals of Astrodynamics*, Dover Publications, N.Y., 1971.
[29] Mehra, R. K., "A Comparison of Several Nonlinear Filters for Reentry Vehicle Tracking," *IEEE Transactions on Automatic Control*, Vol. AC-16, No. 4, pp. 307-319, August 1971.
[30] Miller, R. M., *A Lower Bound on Angle-Only Tracking Accuracy*, MIT Lincoln Laboratory Project Report RMP-149, 9 May 1978.
[31] Lu, S., and Doerschuk, P. C., "Performance Bounds for Nonlinear Filters," *IEEE Transactions on Aerospace and Electronic Systems*, Vol. AES-33, No. 1, pp. 316-318, January 1997.
[32] Tichavsky, P., Muravchik, C., Nehorai, A., "Posterior Cramer-Rao Bounds for Adaptive Discrete-Time System Identification and Nonlinear Filtering," *IEEE Transactions on Signal Processing*, to appear in 1998.
[33] Washburn, R. B., Allen, T. G., Teneketzis, D., "Performance Analysis for Hybrid State Estimation Problems," *Proceedings of American Control Conference*, pp. 1047-1053, 1985.
[34] Muder, D. J., "Cramer-Rao Bound Applied to Single-Target Tracking in a Cluttered Environment (U)," MITRE Technical Report No. MTR 93B0000011, Bedford, MA, 1993 (Unclassified).
[35] Kerr, T. H., "Assessing and Improving the Status of Existing Angle-Only Tracking (AOT) Results," *Proceedings of Sixth International Conference on Signal Processing Applications & Technology (ICSPAT)*, Boston, MA, pp. 1574-1587, 24-26 Oct. 1995.
[36] Siouris, G. M., Chen, G., Wang, J., "Tracking an Incoming Ballistic Missile Using an Extended Interval Kalman Filter," *IEEE Transactions on Aerospace and Electronic Systems*, Vol. AES-33, No. 1, pp. 232-240, January 1997.
[37] Chen, G., Wang, J., Shieh, L. S., "Interval Kalman Filtering," *IEEE Transactions on Aerospace and Electronic Systems*, Vol. AES-33, No. 1, pp. 250-259, January 1997.
[38] Carvalho, H., Del Moral, P., Monin, A., Salut, G., "Optimal Nonlinear Filtering in GPS/INS Integration," *IEEE Transactions on Aerospace and Electronic Systems*, Vol. AES-33, No. 3, pp. 835-840, July 1997.
[39] Widnall, W. S., "Enlarging the Region of Convergence of Kalman Filters Employing Range Measurements," *AIAA Journal*, Vol. 11, No. 3, pp. 283-287, March 1973.
[40] Satz, H. S., Cox, D. B., Beard, R., and Landis, P., "GPS Inertial Attitude Estimation Via Carrier Accumulated Phase Measurements," *Navigation: Journal of the Institute of Navigation*, Vol. 38, No. 3, pp. 273-284, Fall 1991.
[41] Kerr, T. H., "Decentralized Filtering and Redundancy Management for Multisensor Navigation," *IEEE Trans. on Aerospace and Electronic Systems*, Vol. AES-23, No. 1, pp. 83-119, Jan. 1987 (minor corrections appear on p. 412 of May and on p. 599 of July 1987 issues of same journal) [won 1988 M. Barry Carlton Award for Best AES Paper in 1987].
[42] Kerr, T. H., *Cramer-Rao Lower Bound Implementation and Analysis: CRLB target tracking evaluation methodology for NMD radars*, MITRE Technical Report MTR No. 98B0000035, Bedford, MA, February 1998.
[43] Kerr, T. H., "Computational Techniques for the Matrix Pseudo-inverse in Minimum Variance Reduced-Order Filtering and Control," in *Control and Dynamic Systems-Advances in Theory and Applications*, Vol. XXVIII: Advances in Algorithms and computational Techniques for Dynamic Control Systems, Part 1 of 3, C. T. Leondes (Ed.), Academic Press, NY, 1988.
[44] Brown, C. D., Spacecraft Mission Design, AIAA Education Series, 1992.
[45] Kouritzin, M. A., "On Exact Filters for Continuous Signals with Discrete Observations," *IEEE Transactions on Automatic Control*, Vol. 43, No. 5, pp. 709-714, May 1998.
[46] Kerr, T. H., "Fallacies in Computational Testing of Matrix Positive Definiteness/Semidefiniteness," *IEEE Transactions on Aerospace and Electronic Systems*, Vol. AES-26, No. 2, pp. 415-421, March 1990.
[47] Gini, F., "A Radar Application of a Modified Cramer-Rao Bound: Parameter Estimation in Non-Gaussian Clutter," *IEEE Transactions on Signal Processing*, Vol. 46, No. 7, pp. 1945-1953, July 1998.
[48] Kerr, T. H., "Extending Decentralized Kalman Filtering (KF) to 2-D for Real-Time Multisensor Image Fusion and/or Restoration: Optimality of Some Decentralized KF Architectures," *Proceedings of ICSPAT*, Boston, MA, 10-12 Oct. 1996.